Journal of Chromatography A, 1511 (2017) 59–67

Contents lists available at ScienceDirect

Journal of Chromatography A

journal homepage: www.elsevier.com/locate/chroma

Quantitative characterization of gold nanoparticles by size-exclusion and hydrodynamic chromatography, coupled to inductively coupled plasma mass spectrometry and quasi-elastic light scattering

Leena Pitkänen[1], Antonio R. Montoro Bustos, Karen E. Murphy, Michael R. Winchester*, André M. Striegel*

Chemical Sciences Division, National Institute of Standards and Technology (NIST), 100 Bureau Drive, Gaithersburg, MD 20899, USA

ARTICLE INFO

Article history:
Received 14 February 2017
Received in revised form 21 June 2017
Accepted 23 June 2017
Available online 27 June 2017

ABSTRACT

The physicochemical characterization of nanoparticles (NPs) is of paramount importance for tailoring and optimizing the properties of these materials as well as for evaluating the environmental fate and impact of the NPs. Characterizing the size and chemical identity of disperse NP sample populations can be accomplished by coupling size-based separation methods to physical and chemical detection methods. Informed decisions regarding the NPs can only be made, however, if the separations themselves are quantitative, *i.e.*, if all or most of the analyte elutes from the column within the course of the experiment. We undertake here the size-exclusion chromatographic characterization of Au NPs spanning a six-fold range in mean size. The main problem which has plagued the size-exclusion chromatography (SEC) analysis of Au NPs, namely lack of quantitation accountability due to generally poor NP recovery from the columns, is overcome by carefully matching eluent formulation with the appropriate stationary phase chemistry, and by the use of on-line inductively coupled plasma mass spectrometry (ICP-MS) detection. Here, for the first time, we demonstrate the quantitative analysis of Au NPs by SEC/ICP-MS, including the analysis of a ternary NP blend. The SEC separations are contrasted to HDC/ICP-MS (HDC: hydrodynamic chromatography) separations employing the same stationary phase chemistry. Additionally, analysis of Au NPs by HDC with on-line quasi-elastic light scattering (QELS) allowed for continuous determination of NP size across the chromatographic profiles, circumventing issues related to the shedding of fines from the SEC columns. The use of chemically homogeneous reference materials with well-defined size range allowed for better assessment of the accuracy and precision of the analyses, and for a more direct interpretation of results, than would be possible employing less rigorously characterized analytes.

Published by Elsevier B.V.

1. Introduction

Over the past two decades, the applications of nanomaterials in both fundamental research and applied science have proliferated. Gold nanoparticles (Au NPs), in particular, have found a rapidly growing range of uses. These latter include as connectors in nanoelectronics chips [1]; for photodynamic therapy, *e.g.*, hyperthermia therapy wherein the infrared heating of nanoparticles contained in a tumor serves to kill the tumor cells [2]; for the delivery of therapeutic agents, capitalizing upon the large surface area to volume ratio of the Au NPs [3]; as sensors for proteins, pollutants, and food contaminants [4]; in biological imaging, as transmission electron microscopy probes [5]; for the detection of biomarkers related to various diseases and infectious agents [6]; in home pregnancy tests based on lateral flow immunoassays [7,8]; and as catalysts [9], to name but a few.

Accompanying the above applications is a variety of concerns regarding the environmental and physiological impact of Au NPs. Covered extensively in a number of relatively recent publications [10–12], these include accumulation in both biological tissues (gut biota, cell nuclei, *etc.*) and in estuarine mesocosms [11,13]; the upregulation of antioxidants, stress response genes, and protein expression (*e.g.*, induced oxidative stress in the digestive gland of bivalves) [14,15]; reduction of human sperm motility [16]; *etc.* Bio- and econanotoxicity effects for nanoparticulate gold have found to be size dependent, with the kinetics of intracellular uptake dif-

* Corresponding authors.
E-mail addresses: mwinchester@nist.gov (M.R. Winchester), andre.striegel@nist.gov (A.M. Striegel).
[1] Current address: Department of Food and Environmental Sciences, University of Helsinki, P.O. Box 66, Helsinki, 00014, Finland.

http://dx.doi.org/10.1016/j.chroma.2017.06.064
0021-9673/Published by Elsevier B.V.

fering markedly among 14 nm, 50 nm, and 74 nm Au NPs; and with 10 nm Au NPs found in the blood and certain organs of male Wistar-derived rats, while larger Au NPs were not found in many of the same organs [17]. Shape has also been found to play a role, with Au nanorods displaying cytotoxic effects where Au NPs do not [18]; and with HaCaT cells incubated with Au nanorods and nanoprisms displaying different bright field confocal miscroscope images, indicative of differences in cellular uptake, than do cells incubated with Au NPs [12,19].

Given the important role that size plays in both the application and the fate of Au NPs, its characterization is paramount. For narrowly distributed NP size populations, this has generally been done employing off-line quasi-elastic light scattering (QELS, also known as dynamic light scattering), transmission electron microscopy and, more recently, single particle inductively coupled plasma mass spectrometry. For more broadly distributed samples, multimodal samples, or in the case of blends, separation techniques are needed and these have included, in the case of Au NPs, size-exclusion chromatography (SEC) [20] hydrodynamic chromatography (HDC) [21–25], field-flow fractionation (FFF) [21,26–30], and both gel and capillary electrophoresis [31]. Each of these techniques has its own advantages and disadvantages relative to the others and, while a discussion of this is beyond the topic of the present contribution, a number of comparisons have appeared in the recent literature [32–36].

As pointed out in a recent review [37], one issue which has plagued the SEC characterization of NPs over the last quarter century has been a lack of quantitation accountability, *i.e.,* NP recoveries from columns are, with very few exceptions [see *e.g.*, [21,22,38]], not reported. This information gap naturally generates uncertainty with respect to how much, or which portion, or both, of the sample has actually been characterized. One way in which this failure has been overcome, in both the HDC and asymmetric flow FFF (AF4) characterization of nanoparticles, has been through the use of inductively coupled plasma mass spectrometry (ICP-MS) as a detection method following the separations [20–35,39–41]. ICP-MS is an elemental-specific tool which can quantitate metals with high sensitivity. When coupled to separation techniques such as HDC or AF4, multi-element size profiles can be obtained with a single run. Because high sensitivity is necessary especially when environmental samples with low NP/metal concentrations are analyzed, an additional attractive feature of ICP-MS is that, coupled to a separation technique, it enables the detection of nanoparticles in the ng g^{-1} range in suspension [21,42,43]. Thus, ICP-MS provides more sensitivity over other commonly used (in macromolecular and NP separations) spectroscopic detection methods such as ultraviolet or light scattering photometry or refractometry [44]. Recovery quantification when using on-line ICP-MS is accomplished *via* the use of dose-response calibration curves. The ICP-MS thus plays a dual role: That of mass-selective element detector [45,46], providing information on the metal(s) present in the NP, and as a sensitive mass fraction detector, informing our knowledge of analyte column (or channel, in the case of AF4) recovery.

Here, we compare the separation of Au NPs employing both SEC/ICP-MS and HDC/ICP-MS, as well as HDC/QELS. The study of binary and ternary Au NP blends is investigated; column recoveries, determined using the on-line mass spectrometry detector, are (a) reported and (b) shown to be quantitative, averaging over 95% by each method (collectively, these two features, (a) and (b), correspond to a "quantitative characterization" of the materials involved); and a comparison among two different size-based separation methods (SEC and HDC) which employ the same type of column chemistry as each other is given. Additionally, the use of chemically homogeneous, stable, reference materials (RMs) with well-defined size ranges allows for a better assessment of the accuracy and precision of the analyses, for a more direct interpretation of measurements and results, and for a better informed interpretation of possible sources of experimental variability, than are normally possible when analyzing non-RM samples [47]. The latter type of analytes is planned as the subject of future studies.

Table 1
Experimental conditions for the ICP-MS detection in SEC/ICP-MS and HDC/ICP-MS analyses.

Plasma conditions		
RF Power applied (W)		1400
Plasma gas flow (L min^{-1})		13
Sample gas flow (L min^{-1})		0.90
Nebulizer gas flow (L min^{-1})		0.94
Extraction (V)		− 350
Hexapole bias (V)		− 4.0
Quadrupole bias (V)		−1.1
Data acquisition parameters		
Acquisition mode	Time Resolved Analysis	
Monitored isotopes	^{197}Au, ^{115}In	
Dwell time (ms)	300	

2. Experimental

2.1. Materials

Three gold nanoparticle (Au NP) reference materials (RMs) with approximately spherical shape and with nominal diameters of 10 nm, 30 nm, and 60 nm, were obtained from NIST (RM 8011, RM 8012 and RM 8013, respectively, Gaithersburg, MD, USA) [48–50]. The Au NPs are stabilized with citrate and supplied as suspensions in water. NIST Standard Reference Material (SRM) 3121 Gold (Au) Standard Solution was used as ionic gold; NIST SRM 3124a Indium (In) Standard Solution was used as an internal standard [51]. Milli-Q (Millipore, Billerica, MA, USA) high-purity water was used for all sample preparations and dilutions. Concentrated nitric acid (69%, mass fraction) and hydrochloric acid (32% to 38%, mass fraction) were from GFS Chemicals (Veritas double distilled, Columbus, OH, USA). Sodium hydrogen phosphate (Na_2HPO_4), Triton X-100, and sodium dodecyl sulphate (SDS) were from Sigma-Aldrich (St. Louis, MO, USA). Formaldehyde was purchased from Mallinckrodt Chemicals (Paris, KY, USA).

2.2. SEC/ICP-MS

Separation of Au NPs was conducted using an SEC instrument which consisted of a Varian 9012 pump (Palo Alto, CA, USA), a Wyatt high-pressure injection system with 100 μL loop (Wyatt Technology Corp., Santa Barbara, CA, USA), and a bank of two 8.0 mm × 300 mm MCX columns from PSS Polymer Standards Service (Mainz, Germany) with 10^6 and 10^3 Å nominal pore sizes and 10 μm diameter sulfonated styrene/divinyl benzene copolymer particles. A Thermo Fisher X-Series 7 quadrupole inductively coupled plasma mass spectrometer (Thermo Fisher Scientific, Waltham, MA, USA) was directly coupled to the SEC system for elemental detection. The ICP-MS instrument was equipped with a microflow perfluoroalkoxy (PFA) concentric nebulizer (PFA-ST, Elemental Scientific, Omaha, NE, USA) and an impact bead spray chamber cooled to 2 °C. To minimize the matrix influence on the ICP-MS signal, a Xi skimmer Ni cone (Thermo Fisher Scientific) was used throughout for ICP-MS measurements. The experimental conditions for ICP-MS detection are summarized in Table 1.

The mobile phase used for both the SEC/ICP-MS and HDC/ICP-MS analyses was 0.5 mmol L^{-1} Na_2HPO_4 + 0.05% Triton X–100 + 0.013% SDS + 0.05% formaldehyde, pH 7.5 (all percentages are mass based, the balance of the mass being water). This is a variant of the HDC eluent formulation of McGowan and Langhorst [52], which our

group has previously employed successfully in the multi-detector HDC analysis of particles with a variety of shapes and sizes [53–55]. The choice of eluent, along with that of SEC and HDC column packing material, is discussed in the Supporting Information, along with the role of the various eluent components in preventing analyte aggregation in solution and analyte adsorption onto the columns. Indium (0.1 ng g^{-1}) was added to the mobile phase to monitor the signal level at mass-to-charge ratio (m/z) 115 to correct for signal drift and matrix effects. Before analyses, the instrument was tuned daily using a multi-element standard solution (1 μg L^{-1} of each of Li, Be, Co, In, Ba, Ce, and U in 2% v/v nitric acid) for maximum ^{115}In sensitivity and minimum oxide (^{156}CeO/^{140}Ce) level (<2%). Under this condition, the ICP-MS also exhibited maximum sensitivity for ^{197}Au. Flow rates of 0.25 mL min^{-1}, 0.5 mL min^{-1}, and 1 mL min^{-1} were employed.

All samples and working standard solutions were prepared on a mass fraction basis. Au NPs were suspended in the mobile phase at a final Au mass fraction between 10 ng g^{-1} and 100 ng g^{-1}. For the recovery calculations, calibration curves were prepared using the 10 nm diameter Au NP and also the ionic Au standard. Flow injection analysis was used to directly inject both species to the ICP-MS (without SEC separation, but using the same flow rate as in SEC) using mass fractions ranging between 1 ng g^{-1} and 50 ng g^{-1}. Five sequential injections were made of each solution and the average peak areas were employed to construct the calibration curve (peak area versus mass fraction). Origin 2015 graphing software (v. 9.1, OriginLab, Northampton, MA, USA) was used for all integrations and peak area calculations.

2.3. HDC/ICP-MS

HDC/ICP-MS analyses were performed using the same instrumentation and mobile phase as for SEC/ICP-MS, except that the SEC columns were replaced with a bank of two 7.5 mm × 400 mm Agilent/Polymer Laboratories PS-1 HDC columns packed with 15 μm non-porous particles (Agilent/Polymer Laboratories, Amherst, MA, USA). While the HDC mobile phase was unintentionally overspiked with 0.1 μg g^{-1} of In internal standard, this turned out to have a negligible effect on the calculated relative ICP-MS intensities of the various peaks of the individual Au NPs and of the Au NP binary blends. The flow rates employed were 0.5 mL min^{-1} and 1 mL min^{-1}. Column recoveries were determined the same way as described above for SEC.

2.4. HDC/QELS

Independent of the on-line ICP-MS experiments, on-line HDC/QELS experiments were performed employing an Agilent 1260 isocratic pump and autosampler, two Varian PS-1 HDC columns (same column set as employed in the HDC/ICP-MS section above), and an on-line QELS detector (Wyatt). The QELS measurements were performed at a nominal angle of 108° relative to the incident laser beam. The flow rate was 1 mL min^{-1}. ASTRA software (version 6.1.1.17, Wyatt) was used for data collection and processing. Autocorrelation functions for the various Au NPs can be found in the Supporting Information.

It should be noted that SEC/QELS measurements were also attempted, using the SEC column set described above, but particulate shedding from the columns hampered the ability to obtain adequate signal-to-noise ratios for any of the Au NP peaks, even after extended rinsing of the columns with pH 7.45 sodium phosphate solution. The reason this is a problem is because the particulates, or "fines," being shed from the SEC columns scatter large amounts of light, sufficiently so as to create a noisy enough background that obscures, if not completely occludes the signals from the analytes. To date, commercially available "light scattering friendly" sulfonated styrene/divinyl benzene columns SEC do not appear to exist.

Table 2
Chromatographic resolution (R_s) between 10 nm and 60 nm Au NPs in SEC and HDC, at various flow rates.

Flow-rate (mL min^{-1})	R_s	
	SEC/ICP-MS	HDC/ICP-MS
1	0.62 ± 0.03	0.49 ± 0.05
0.5	0.93 ± 0.02	0.62 ± 0.05
0.25	1.06 ± 0.01	

Uncertainties correspond to one standard deviation based on at least duplicate injections per suspension. R_s values based on chromatograms of individual Au NP samples and calculated using the equation $R_s = \frac{2(V_{R10}-V_{R60})}{W_{b60}+W_{b10}}$, where V_R is the peak retention volume; W_b is the chromatogram base peak width determined by the method of tangents and an exponentially modified Gaussian fit; and 10 and 60 refer to the individual 10 nm and 60 nm Au NPs, respectively [46].

3. Results and discussion

3.1. SEC/ICP-MS of Au NPs

Non-functionalized NIST RM Au NPs with nominal diameters of 10 nm, 30 nm, and 60 nm, as well various binary and ternary blends of these NPs, were separated using SEC coupled online to ICP-MS detection. Analyses of the 10 nm and 60 nm NP and of a 1:1 (w/w) blend of both sizes were performed at three different flow rates, namely 1 mL min^{-1}, 0.5 mL min^{-1}, and 0.25 mL min^{-1}. As can be seen in Fig. 1, changes in flow rate do not appear to affect the retention of the NPs. This observation agrees with SEC theory, where retention is predicted to be governed by the extent of analyte permeation into the pores of the column packing material, not by the rate of permeation [46,56–58]. The effect of flow rate on chromatographic resolution, however, is immediately evident in Fig. 1. At 1 mL min^{-1} (Fig. 1A), the resolution R_s of a blend of 10 nm and 60 nm Au NPs was 0.62 (Table 2). Decreasing flow rate by a factor of two, to 0.5 mL min^{-1}, results in a marked improvement in resolution: The 10 nm and 60 nm Au NP populations are more clearly distinguishable from each other in the blend, and now R_s = 0.93 (a 50% increase; see Table 2). Cutting the flow rate in half once more, to 0.25 mL min^{-1}, brings an even further increase in R_s, to 1.06 (*i.e.*, an additional 12% increase; see Table 2). Given that, at 0.25 mL min^{-1}, if the chromatogram of the blend were bisected at the minimum between the peaks each collected portion would be >98% pure (purer than this, if one were to collect only the portions to the left of the peak apex of the 60 nm Au NP peak and to the right of the 10 nm Au NP peak apex) [46], no further reduction in flow rate was investigated.

It should be noted that the observed increase in R_s with decreasing flow rate, described above, agrees with the kinetic theory of diffusion in SEC. According to this theory, for large analytes (a descriptor which has been shown, empirically, to correspond to a diameter larger than ≈10 nm), band broadening is governed chiefly by stationary (or stagnant) mobile phase mass transfer and by the flow-diffusion coupling of the eddy dispersion and extraparticle mobile phase mass transfer terms of the extended van Deemter equation (for analytes smaller than ≈10 nm, and/or at very low flow rates, the effects of longitudinal diffusion become manifest and may even dominate band broadening in SEC) [46,59]. How these findings contrast with what happens in the HDC analysis of Au NPs is explored later in this paper.

We also note here the assumed absence of sample dispersity (either in size or shape) effects in the separation. In addition to the generally accepted wisdom that slices eluting from SEC or HDC columns are sufficiently narrow so as to be considered monodisperse with respect to size, the virtual absence of size dispersity is

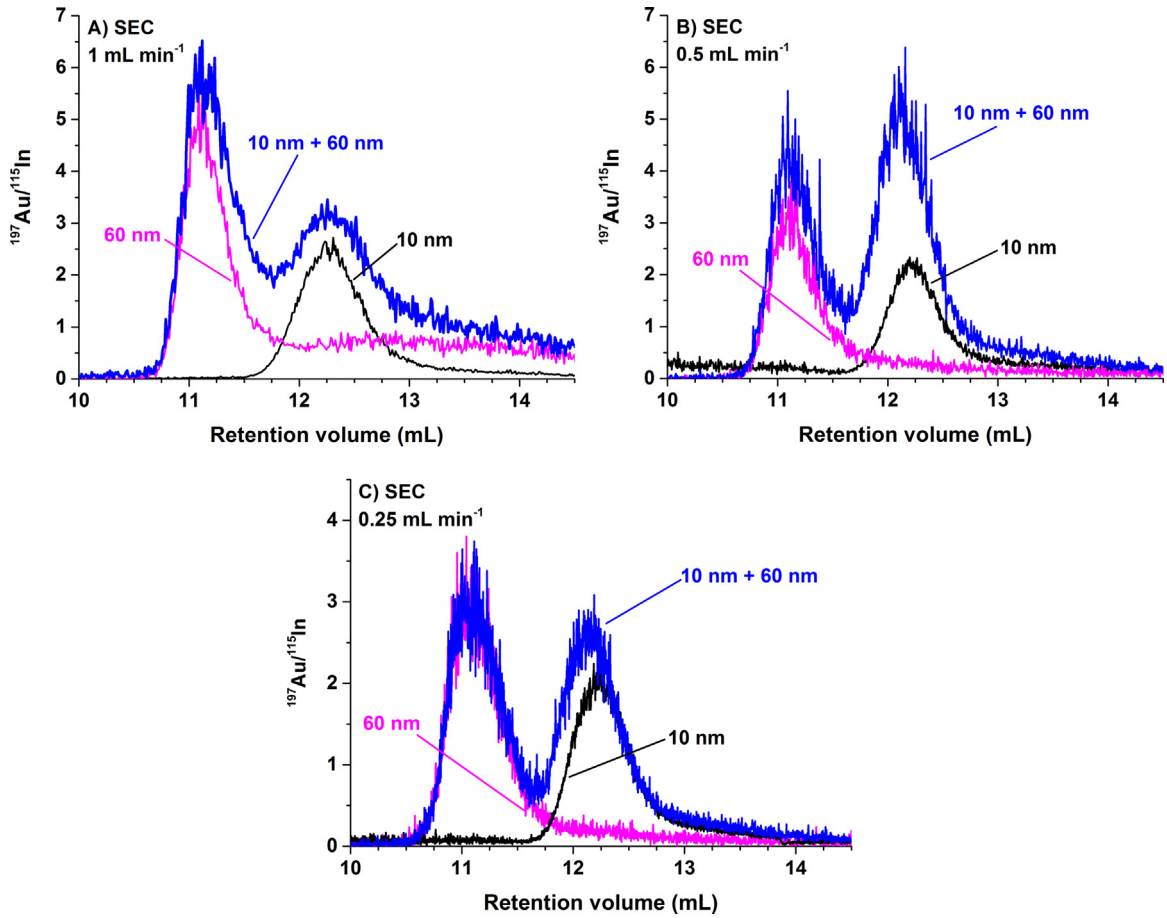

Fig. 1. SEC/ICP-MS chromatograms for individual Au NPs with nominal diameters of 10 nm (black), 60 nm (magenta), and 1:1 (w/w) blend of the two (blue), at three different flow rates, A) 1 mL min^{-1}, B) 0.5 mL min^{-1}, and C) 0.25 mL min^{-1}. The injected mass was 10 ng per individual NP (*i.e.*, for the binary blends, a total of 20 ng of NP was injected, 10 ng each of the 10 nm and the 60 nm Au NP). Note that ordinates in Figs. 1–3 have been normalized for In content in mobile phase (see Experimental for details). (For interpretation of the references to colour in this figure legend, the reader is referred to the web version of this article.)

also evidenced by the fact that the translational diffusion coefficient (D_T) dispersity, defined as the ratio of the weight- to number-average D_T (*i.e.*, as $D_{T,w}/D_{T,n}$), ranges from 0.95 ± 0.02 to 1.01 ± 0.01 for the Au NPs examined. Here, D_T was measured at each slice eluting from the HDC columns using quasi-elastic light scattering (QELS) detection, as described more fully in Sections 2.4 and 3.3. As regards shape dispersity, which can lead to so-called local polydispersity effects (*i.e.,* to the coelution of samples of different shape but which occupy the same hydrodynamic volume in solution), the scanning electron and transmission electron microscopy data in references [48–50] are clear evidence that this is not an issue, because all three Au NPs were demonstrated to be homogenous and virtually spherical with respect to shape.

In addition to the binary NP blend, a ternary 1:1:1 (w/w/w) blend of the 10 nm, 30 nm, and 60 nm Au NPs was also analyzed by SEC. The result of the analysis, which was performed at 0.25 mL min^{-1}, is shown in Fig. 2. As can be seen in the figure, as the relative size difference between Au NPs increases, so does the chromatographic resolution: The R_s between the individual 30 nm and 60 nm particles, which differ from each other in size by only a factor of 2, is 0.41, whereas the R_s between the 10 nm and 30 nm Au NPs (relative size difference of 3) is 0.57 and, as noted above, for the 10 nm and 60 nm Au NPs, where the size difference has increased to a factor of 6, R_s = 1.06.

In Fig. 2, as is also the case in Figs. 1 and 3 and , an increase in noise is observed in the chromatograms of the individual NPs as a function of increasing NP size. This is due to the fact that, because

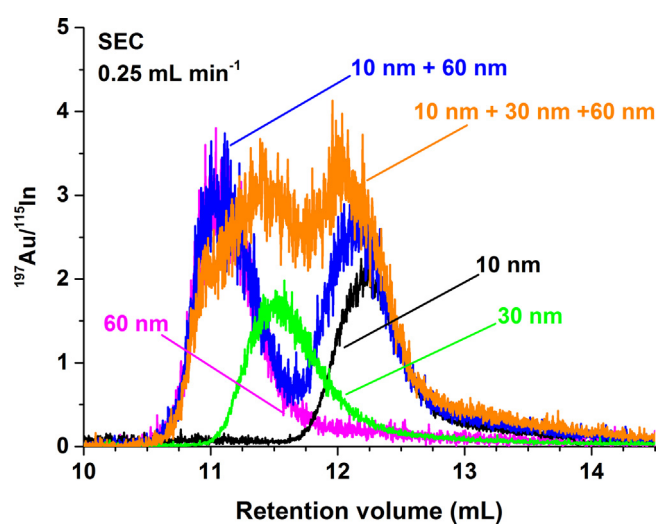

Fig. 2. SEC/ICP-MS chromatograms, obtained at 0.25 mL min^{-1}, of individual Au NPs with nominal diameter of 10 nm (black), 30 nm (green), 60 nm (magenta), of a 1:1 (w/w) blend of the 10 nm and 60 nm Au NPs (blue), and of a 1:1:1 (w/w/w) blend of all of the three NPs (orange). In each case, the injected mass followed the convention described in the legend for Fig. 1. (For interpretation of the references to colour in this figure legend, the reader is referred to the web version of this article.)

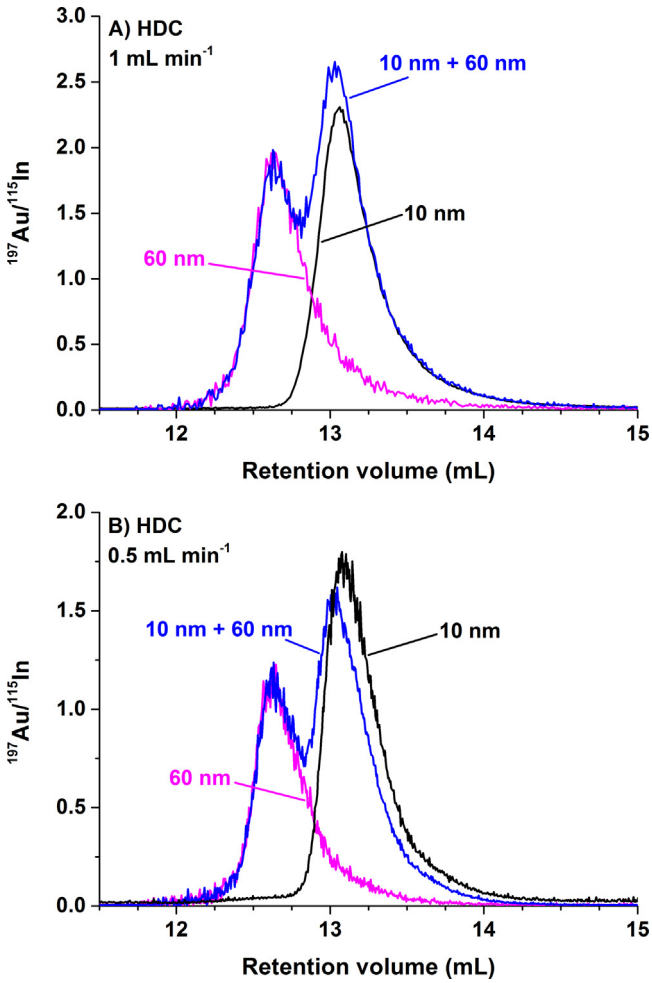

Fig. 3. HDC/ICP-MS chromatograms of Au NPs with nominal diameter of 10 nm (black), 60 nm (magenta), and a 1:1 (w/w) blend of both (blue) obtained employing flow rates of A) 1 mL min^{-1} and B) 0.5 mL min^{-1}. In B), chromatogram of 10 nm NP has been scaled to account for differences in ^{115}In content in solutions of this NP, as compared to solutions of the 60 nm NP or of the blend. (For interpretation of the references to colour in this figure legend, the reader is referred to the web version of this article.)

equal masses of gold were injected onto the columns for each size, the number concentration of 60 nm Au NP is lower than that of the 30 nm Au NP which, in turn, is lower than that of the 10 nm Au NP.

3.2. HDC/ICP-MS of Au NPs and comparison to SEC/ICP-MS

As mentioned in the Introduction, various examples of quantitative HDC/ICP-MS analysis of metal-containing NPs have appeared in the recent literature. HDC is a separation technique which, coupled to a multiplicity of detection methods, has been widely employed for the characterization of polymers, colloids, nanoparticulate drug delivery vesicles, *etc.* [53–55,60–64]. As such, a comparison between SEC/ICP-MS and HDC/ICP-MS, as regards the quantitative separation of Au NPs, appears appropriate. In the present case, the comparison can be made more direct by the fact that both the SEC and the HDC columns used in the experiments employ the same type of packing particle chemistry, namely sulfonated styrene/divinyl benzene, the main difference being that the SEC column packing material is porous, whereas the HDC packing material is not.

Results of the HDC/ICP-MS analysis of the 10 nm and 60 nm particles, both individually and in a 1:1 (w/w) blend, are shown in Fig. 3. Analyses were performed at two different flow rates, 1 mL min^{-1} and 0.5 mL min^{-1}. The R_s values at these flow rates were 0.49 and 0.62, respectively (Table 2, again based on chromatograms of the individual Au NPs). These results merit comparison to each other, as well as to the R_s values obtained during SEC analysis, above.

First, when comparing the R_s of the HDC separations to those of the SEC separations it can be observed in Table 2 that, for a given flow rate (be it 0.5 mL min^{-1} or 1 mL min^{-1}), resolution is better in SEC than in HDC. The higher R_s of the SEC separations, as compared to HDC, is mainly due to the fact that, in HDC, separation occurs through the selective sampling by the analytes of the streamlines of flow in the rather limited interstitial (interparticle) volume of the columns [61]. Conversely, in SEC separation is achieved by the analytes sampling the more abundant intraparticle pore volume [46]. As such, all other factors being equal (or similar, because the SEC and HDC columns do not have the exact same dimensions as each other), higher resolution is expected from SEC separations as compared to HDC.

The flow rate dependence of R_s in SEC has been noted and explained above. As seen in Table 2, however, in HDC flow rate has only a moderate effect on R_s. In HDC, R_s was observed to increase by only 0.13 (a mere 27% increase) with a two-fold decrease in flow rate from 1 mL min^{-1} to 0.5 mL min^{-1} whereas, for the same flow rate change in SEC, R_s increased by 0.31 (a 50% increase). While this marked difference between the chromatographic resolution of two packed column size-based separation methods may seem surprising, the results are in full agreement with what is predicted by the kinetic theory of HDC (see Sections 4 and 5 of ref. [61]). According to this theory, for reduced velocities (which are, by definition, dimensionless) greater than 5 the reduced plate height changes little in HDC (at reduced velocities lower than 5, longitudinal diffusion effects become more manifest in the separation) [61,65]. As such, the relative flow rate independence of R_s in HDC is not unexpected. This means that improvements in HDC resolution can generally only be achieved through reductions in column packing particle size, though it also means that HDC analyses can be performed at relatively high reduced velocities without a sacrifice in chromatographic resolution (assuming no analyte degradation at the increased strain rates that accompany high separation velocities, or that the aspect ratio of the analyte, *i.e.,* the ratio between the effective radius of the analyte and the hydraulic radius of the column, is not so large as to disturb the interparticle Poiseuille flow profile away from its expected parabolic shape) [61].

It is as a consequence of the low resolution of HDC, as exemplified in Fig. 3, that the separation of a ternary blend of 10 nm, 30 nm, and 60 nm NPs was not attempted, whereas the relative flow-rate-independence of HDC R_s explains why flow rates lower than 0.5 mL min^{-1} were not employed in these experiments.

3.3. Size determination of Au NPs by HDC/QELS, and comparison to HDC/ICP-MS

Because the ICP-MS is a mass detector for the atoms from the metallic core of NPs, SEC/ICP-MS and HDC/ICP-MS are valuable tools for element-specific characterization of (colloidal) samples containing NPs. However, neither of these chromatographic/mass spectrometric couplings provides direct information on NP size (unless, that is, the ICP-MS is operated in single particle mode [22,23,66–68], which is not the case here). On-line coupling of quasi-elastic light scattering (QELS) detection to size-based separation techniques such as SEC or HDC provides a method by which to determine hydrodynamic particle size continuously across the NP chromatograms, without having to rely on constructing and applying NP diameter calibration curves. Because of chromatographic (and extracolumn) band broadening of analyte peaks in SEC and HDC, the calibration curve approach tends to overestimate the size

range of the sample [37,69]. With QELS detection, however, the translational diffusion coefficient D_T of the NPs is measured at each slice eluting from the chromatographic columns [46]. This coefficient is a parameter directly relatable to NP size, with the relation between D_T and the hydrodynamic (Stokes) radius R_H given by [45,46,70,71]:

$$R_H \equiv \frac{k_B T}{6\pi\eta_0 D_T} \quad (1)$$

where k_B is Boltzmann's constant, T is the absolute temperature of the experiment, and η_0 is the solvent or carrier fluid viscosity at the experimental temperature. (R_H is generally interpreted as the radius of a homogeneous hard sphere, *i.e.,* of a sphere of constant density and composition, which has the same D_T as the analyte. Given the aforementioned sphericity and chemical homogeneity of the Au NPs, this equivalency can, in the present case, be considered an equality). Consequently, with on-line QELS detection it is possible to measure size, by way of R_H, continuously across the NP chromatograms.

As mentioned earlier, successful coupling of the SEC columns employed in this experiment to QELS detection was not possible, due to excessive shedding of "fines" by these columns, even after extensive flushing. Shedding was not an issue with the HDC columns used, however. Results of the HDC/QELS experiments are shown in Fig. 4. The two smallest Au NPs (nominal diameters of 10 nm and 30 nm) are seen to have the narrowest size distribution, as exemplified by the R_H of these analytes being relatively constant across the HDC chromatograms. This agrees with results from previous TEM, off-line QELS, and related characterization of these materials [48–50]. For example, the 60 nm diameter Au NP is observed in Fig. 4C to have the broadest distribution of R_H values, from ≈18 nm to ≈48 nm, in excellent agreement with previous TEM analysis which showed the radius of this NP to span the range from ≈22 nm to ≈43 nm [50]. An inversion in HDC elution order is observed, however, in Fig. 4C for the 60 nm Au NP. While at present we cannot state with certainty why this inversion occurs, wherein larger NPs elute after smaller ones for retention volumes greater than ≈13.1 mL, given the size of this NP relative to the hydraulic radius of the HDC columns (≈3 μm), we can rule out both disturbances of the interstitial Poiseuille flow away from its parabolic profile as well as the mechanical entrainment of NPs within the column [53,61]. Rather, excessive enthalpic interactions between the larger NPs in this sample and the column packing material are likely responsible for the behavior observed, with the solution translational entropy ΔS^{trans} of these larger components no longer being the primary governing force for their HDC separation [61]. It is an added benefit of on-line QELS detection that it is able to provide evidence of this type of non-HDC behavior during the separation process.

When comparing the HDC/ICP-MS chromatograms, at a flow rate of 1 mL min^{-1}, of the 10 nm and 60 nm Au NPs (Fig. 3A) to the HDC/QELS chromatograms of the same NPs at the same flow rate (Figs. 4A,C), a few features stand out. First, when employing QELS detection, the chromatogram of the smaller NP is substantially noisier than when ICP-MS detection is employed. This is not surprising, given that light scattering intensity is directly proportional to the molar mass and size of the scattering object, *i.e.,* smaller objects or lower molar mass ones will scatter less light than will their larger, higher molar mass counterparts. Consequently, all other things being equal, light scattering signal-to-noise ratio (S/N) decreases with decreasing analyte size and molar mass. This is not the case for ICP-MS, however, because it is a mass-sensitive detector that is unbiased with respect to analyte size and/or molar mass. With the 60 nm Au NP, the opposite situation exists. Given this NPs larger size, its HDC/QELS chromatogram is fairly "clean," characterized by a high S/N due to increased scattering intensity.

Table 3
Column recoveries (given as percentage of injected amount) from SEC/ICP-MS and HDC/ICP-MS analyses (see Experimental – SEC/ICP-MS for details).

	SEC/ICP-MS[c]	HDC/ICP-MS[d]
10 nm[a]	134 ± 10	124 ± 8
30 nm[a]	108 ± 3	93 ± 4
60 nm[a]	85 ± 2	98 ± 2
Au ionic[b]		99 ± 2

[a] Determined using 10 nm Au NP as a standard.
[b] Determined using ionic Au as a standard.
[c] Flow-rate 0.25 mL min^{-1}.
[d] Flow-rate 1 mL min^{-1}.

Second, we observe that the 1 mL min^{-1} HDC/ICP-MS chromatogram of the 60 nm Au NP is less symmetric than is the corresponding HDC/QELS chromatogram: The peak asymmetry factor (in both cases calculated at 10% peak height) is 2 by HDC/ICP-MS, but is only 1.75 by HDC/QELS. While more symmetric, the HDC/QELS chromatogram of this NP is also broader, covering an elution range of ≈3.1 mL, as compared to a range of only ≈1.67 mL by HDC/ICP-MS. We believe this is partly due to the difference in the amount of sample injected, 5 μg in HDC/QELS versus 10 ng in HDC/ICP-MS, and partly due to the abovementioned non-ideal HDC elution behavior observed for the 60 nm Au NP. The fact that the latter effect causes large NPs to elute late in the chromatogram, and the fact that (as noted in the previous paragraph) large, high molar mass species scatter light at a higher intensity than do smaller, lower molar mass species, combine to increase the sensitivity of QELS detection for this NP in the late elution region of the chromatogram. Given that this increase in sensitivity is absent in ICP-MS detection, the HDC/QELS chromatogram is broader than is the HDC/ICP-MS one.

Last, and largely due to the peak width differences noted in the previous paragraph, chromatographic resolution between the 10 nm and 60 nm Au NP chromatograms, at 1 mL min^{-1}, is greater by HDC/ICP-MS, where R_s = 0.49 (see Table 2), than it is by HDC/QELS, where the R_s is only 0.34.

3.4. Quantitation of Au NP recovery in SEC/ICP-MS and HDC/ICP-MS

As mentioned in the Introduction, the SEC literature on nanoparticles is conspicuous for its general absence of reported column recovery values [37]. This knowledge gap makes it difficult, if not impossible, to assess the accuracy of the analyses performed, as it is unknown how much of the sample was characterized or, if only a portion of the sample was characterized, whether this portion is representative of the sample as a whole. Here, the use of on-line ICP-MS detection allowed determination of SEC and HDC column recoveries. This was done by applying mass fraction calibration curves constructed with both the 10 nm Au NP as well as with ionic Au, with the mass spectrometer decoupled from the separation systems, but employing the same flow rates as in the on-line experiments by flow injection analysis. Details are given in the Experimental – SEC/ICP-MS section.

To determine whether the NPs have irreversibly sorbed onto the column packing material, the above-mentioned mass fraction calibration curves were applied to the on-line ICP-MS data to quantitate column recovery. Recovery results for the individual analytes, by each of the chromatographic methods (SEC and HDC), are given in Table 3. For SEC at 0.25 mL min^{-1} (where the best resolution was obtained among the examined flow rates), the percent recovery from the columns was determined to be (109 ± 24) % as averaged over all individual analytes. For HDC at 1 mL min^{-1}, recovery was (104 ± 14) % (for both methods, n ≥ 2 of each, total n ≥ 6). In both cases, analyses can be considered quantitative, with recov-

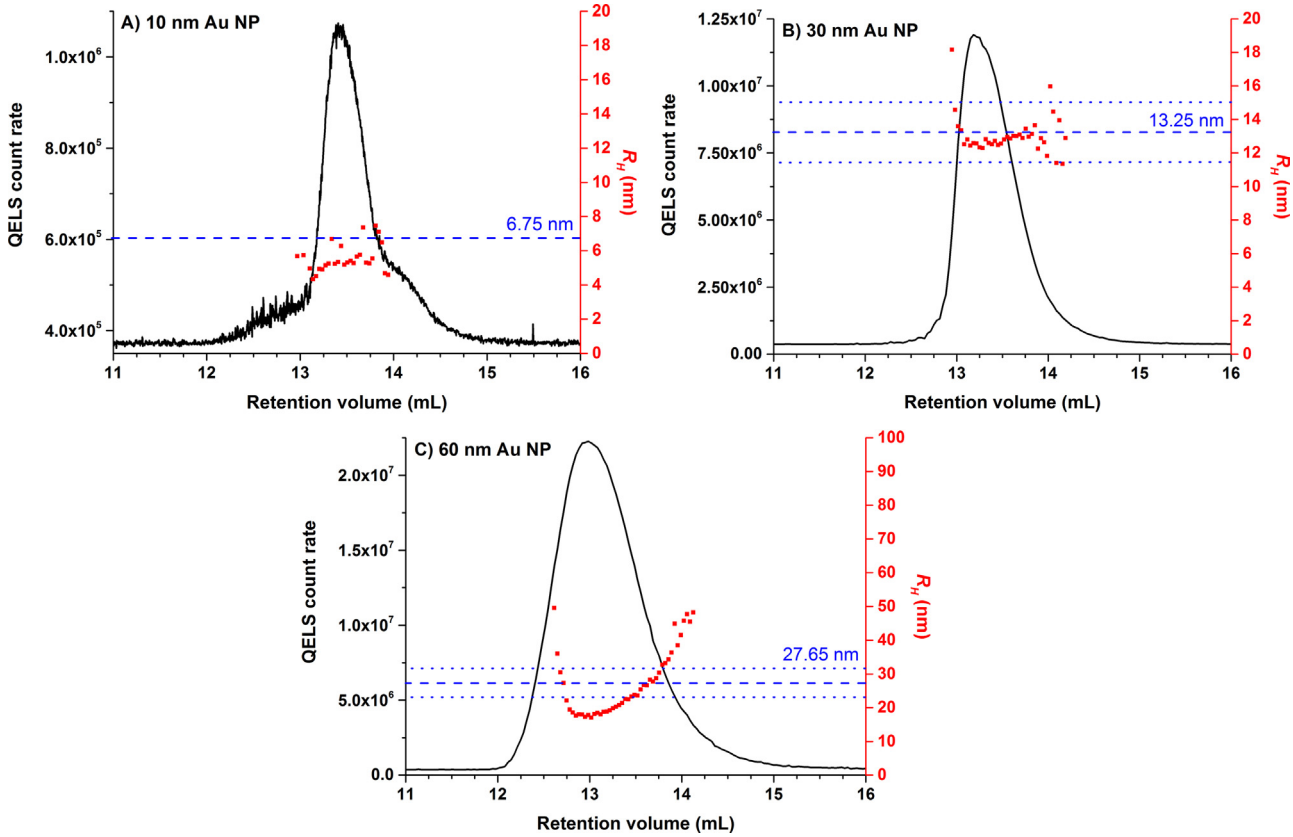

Fig. 4. HDC/QELS chromatograms (black lines) of Au NPs with nominal diameters of A) 10 nm, B) 30 nm, and C) 60 nm. Hydrodynamic radius (R_H) obtained with on-line QELS is plotted across the peaks in each chromatogram (red squares). Mean radii by off-line QELS (from refs. [48–50] for 10 nm, 30 nm, and 60 nm Au NP, respectively) are plotted as blue dashed lines with numerical mean given above line, with expanded uncertainties as dotted blue lines; expanded uncertainty from the mean is <0.1 nm for the 10 nm Au NPs. Off-line QELS analyses were performed at 90° for the 30 nm and 60 nm Au NPs, at 173° (backscatter) for the 10 nm Au NP. (For interpretation of the references to colour in this figure legend, the reader is referred to the web version of this article.)

ery percentages at the very least equaling those reported in recent HDC/ICP-MS and AF4/ICP-MS publications [20,21,25–27,36,40].

It should also be noted here that the 10 nm Au NP vial was opened some time before the vials of the other samples, allowing for a higher probability of NP aggregation in this solution than in the others. Sampling from what remained in this vial after some time and after several experiments likely meant sampling from a solution with increased sample concentration due to aggregation and the "sedimentation" of aggregates toward the bottom of the vial. This presumed aggregation, previously observed in [72], would also be responsible for the higher recoveries measured for the 10 nm Au NP as compared to the other NPs examined, and was also very recently reported for 10 nm Au NPs by López-Sanz et al. in reversed phase LC/ICP-MS analysis [73]. Not counting the 10 nm Au NP, average recovery by SEC at 0.25 mL min^{-1} is (96 ± 16) % and, by HDC at 1 mL min^{-1}, (97 ± 3) %.

4. Conclusions

Size-exclusion chromatography remains the most popular analytical separation technique for determining the molar mass and size distributions of macromolecules. To date, with certain notable exceptions [20,37,72,73–77], this popularity has not extended to the analysis of nanoparticles, principally because of poor (or unknown, or unreported) analyte recovery from the SEC columns, as a result of irreversible analyte sorption onto the column packing material (generally, silica or non-functionalized polymeric resins). SEC, however, presents a promising alternative to currently favored separation methods such as hydrodynamic chromatography and asymmetric flow field-flow fractionation, due to the range of particle and pore sizes and packing materials available for SEC.

Here, we have demonstrated how on-line interfacing of SEC to ICP-MS allows both for chemical characterization of gold nanoparticles as well as for quantitation of analyte recovery. With proper formulation of carrier fluid, matched with a corresponding choice of column packing material, SEC/ICP-MS was shown to be a quantitative method by which to characterize Au NPs in the range of 10 nm to 60 nm. The SEC/ICP-MS analyses of individual samples, as well as of binary and ternary blends, were compared to HDC/ICP-MS experiments conducted under virtually identical conditions (save for the non-porous nature of the HDC column packing material, as compared to the porous SEC columns). Column recoveries in both types of analysis were complete and at least matched, if not exceeded, most results reported to date using alternative separation methods. Not surprisingly, the chromatographic resolution of SEC proved generally superior to that of HDC, with R_S results at several flow rates for both techniques agreeing with the kinetic theory of separations for each method.

Issues remain regarding the stability of the chosen sulfonated styrene/divinyl benzene SEC columns, especially concerning the shedding of fines, thus precluding the use of on-line light scattering detection to determine *e.g.*, the size of the NPs as a continuous function of their chromatographic elution volume. This obstacle could potentially be overcome by the use of single particle ICP-MS [22,23,78,79], an issue which is currently being investigated in our laboratories. However, given the wealth of information that can be derived from on-line light scattering detectors of both the multi-angle static and quasi-elastic varieties, there remains a need

for more stable SEC columns with this, or related, types of column packing materials. HDC was not subject to this column shedding shortcoming and, by the use of HDC/QELS, which measured the hydrodynamic radius of the Au NPs across the chromatograms, and by comparison with high quality, well characterized, chemically homogeneous RMs with a well-defined size range, we were able to demonstrate close agreement with independently obtained off-line QELS size data.

We believe the results presented here show the strength and potential of SEC/ICP-MS, with proper choice of columns and proper formulation of eluent, as an analytical method for not only Au NPs, but also for other types of nanoparticles (*e.g.,* silver NPs) and quantum dots. Once the ability to couple additional molar-mass-sensitive detectors (*e.g.,* light scattering, viscometry) as part of an on-line train is realized, this should allow for the characterization of NP molar mass, size, shape, and chemistry, continuously across the chromatograms and in fully quantitative fashion. The ability to determine these will impact not only fundamental scientific research, but also help tailor the applications of nanoparticles and help in assessing the environmental impact of these materials.

Disclaimer

The identification of certain commercial equipment, instruments, or materials does not imply recommendation or endorsement by the National Institute of Standards and Technology. These identifications are made only to specify the experimental procedures in adequate detail.

Notes

The authors declare no competing financial interest.

Appendix A. Supplementary data

Supplementary data associated with this article can be found, in the online version, at **http://dx.doi.org/10.1016/j.chroma.2017.06.064**.

References

[1] D. Huang, F. Liao, S. Molesa, D. Redinger, V. Subramanian, Plastic-compatible low resistance printable gold nanoparticle conductors for flexible electronics, J. Electrochem. Soc. 150 (2003) G412–G417.
[2] T. Stuchinskaya, M. Moreno, M.J. Cook, D.R. Edwards, D.A. Russell, Targeted photodynamic therapy of breast cancer cells using antibody-phthalocyanine-gold nanoparticle conjugates, Photochem. Photobiol. Soc. 10 (2011) 822–831.
[3] S.D. Brown, P. Nativo, J.-A. Smith, D. Stirling, P.R. Edwards, B. Venugopal, D.J. Flint, J.A. Plumb, D. Graham, N.J. Wheale, Gold nanoparticles for the improved anticancer drug delivery of the active component of oxaliplatin, J. Am. Chem. Soc. 132 (2010) 4678–4684.
[4] M.E. Ali, U. Hashim, S. Mustafa, Y.B. Che Man, Kh. N. Islam, Gold nanoparticle sensor for the visual detection of pork adulteration in meatball formulation, J Nanomater. 2012 (2012), article ID 136706.
[5] S.D. Perrault, W.C.W. Chan, In vivo assembly of nanoparticle components to improve targeted cancer imaging, Proc. Nat. Acad. Sci. 107 (2010) 11194–11199.
[6] G. Peng, U. Tisch, O. Adams, M. Hakim, N. Shehada, Y.Y. Broza, S. Bilan, R. Abdah-Bortnyak, A. Kuten, H. Haick, Diagnosing lung cancer in exhaled breath using gold nanoparticles, Nature Nanotech. 4 (2009) 669–673.
[7] R. Rojanathanes, A. Sereemaspun, N. Pimpha, V. Buasom, P. Ekawong, V. Wiwanitkit, Gold nanoparticles as an alternative tool for a urine pregnancy test, Taiwan J. Obstet. Gynecol. 47 (2008) 296–299.
[8] See, for example, First Response™ Gold™ Digital Pregnancy Test.
[9] D.T. Thompson, Using gold nanoparticles for catalysis, Nano Today 2 (4) (2007) 40–43.
[10] M.A. Maurer-Jones, I.L. Gunsolus, C.J. Murphy, C.L. Haynes, Toxicity of engineered nanoparticles in the environment, Anal. Chem. 85 (2013) 3036–3049.
[11] C.S. Yah, The toxicity of gold nanoparticles in relation to their physicochemical properties, Biomed. Res.-India 24 (2013) 400–413.
[12] P.C. Ray, H. Yu, P.P. Fu, Toxicity and environmental risks of nanomaterials: challenges and future needs, J. Environ. Sci. Health C 27 (2009) 1–35.
[13] J.L. Ferry, P. Craig, C. Hexel, P. Sisco, R. Frey, P.L. Pennington, M.H. Fulton, I.G. Scott, A.W. Decho, S. Kashiwada, C.J. Murphy, T.J. Shaw, Transfer of gold nanoparticles from the water column to the estuarine food web, Nature Nanotech. 4 (2009) 441–444.
[14] J.J. Li, D. Hartono, C.N. Ong, B.H. Bay, L.Y.L. Yung, Autophagy and oxidative stress associated with gold nanoparticles, Biomaterials 31 (2010) 5996–6003.
[15] S. Tedesco, H. Doyle, G. Redmond, D. Sheehan, Gold nanoparticles and oxidative stress in Mytilus edulis, Marine Environ. Res. 66 (2008) 131–133.
[16] V. Wiwanitkit, A. Sereemaspun, R. Rojanathanes, Effect of gold nanoparticles on spermatozoa: the first world report, Fertil. Steril. 91 (2009) e7–e8.
[17] W.H. De Jong, W.I. Hagens, P. Krystek, M.C. Burger, A.J.A.M. Sips, R.E. Geertsma, Particle size-dependent organ distribution of gold nanoparticles after intravenous administration, Biomaterials 29 (2008) 1912–1919.
[18] Arnida, A. Malugin, H. Ghandehari, Cellular uptake and toxicity of gold nanoparticles in prostate cancer cells: a comparative study of rods and spheres, J. Appl. Toxicol. 30 (2010) 212–217.
[19] S. Wang, L. Wentong, I. Tovmachenko, U.M. Rai, H. Yu, P.C. Ray, Challenge in understanding size and shape dependent toxicity of gold nanomaterials in human skin keratinocytes, Chem. Phys. Lett. 463 (2008) 145–149.
[20] M. Al-Sid-Cheikh, M. Pédrot, M.B.-L. Coz, A. Dia, M. Davranche, C. Neaime, F. Grasset, Robust method using online steric exclusion chromatography-ultraviolet-inductively coupled plasms mass spectrometry to investigate nanoparticle fate and behavior in environmental samples, Anal. Chem. 87 (2015) 10346–10353.
[21] E.P. Gray, T.A. Bruton, C.P. Higgins, R.U. Halden, P. Westerhoff, J.F. Ranville, Analysis of gold nanoparticle mixtures: a comparison of hydrodynamic chromatography (HDC) and asymmetrical flow field-flow fractionation (AF4) couples to ICP-MS, J. Anal. At. Spectrom. 27 (2012) 1531–1539.
[22] S.A. Pergantis, T.L. Jones-Lepp, E.M. Heithmar, Hydrodynamic chromatography online with single particle-inductively coupled plasma mass spectrometry for ultratrace detection of metal-containing nanoparticles, Anal. Chem. 84 (2012) 6454–6462.
[23] D. Rakcheev, A. Philippe, G.E. Schaumann, Hydrodynamic chromatography coupled with single-particle inductively coupled plasma mass spectrometry for investigating nanoparticle agglomerates, Anal. Chem. 85 (2013) 10643–10647.
[24] A. Philippe, G.E. Schaumann, Evaluation of hydrodynamic chromatography coupled with UV-visible, fluorescence and inductively coupled plasma mass spectrometry detectors for sizing and quantifying colloids in environmental media, PLoS One 9 (2014) e90559.
[25] D.J. Lewis, Hydrodynamic chromatography—inductively coupled plasma mass spectrometry with post-column injection capability for simultaneous determination of nanoparticle size, mass concentration and particle number concentration (HDC-PCi-ICP-MS), Analyst 140 (2015) 1624–1628.
[26] T.J. Cho, V.A. Hackley, Fractionation and characterization of gold nanoparticles in aqueous solution: asymmetric-flow field flow fractionation with MALS, DLS, and UV–vis detection, Anal. Bioanal. Chem. 398 (2010) 2003–2018.
[27] H. Hagendorfer, R. Kaegi, J. Traber, S.F.L. Mertens, R. Scherrers, C. Ludwig, A. Ulrich, Application of an asymmetric flow field flow fractionation multi-detector approach for metallic engineered nanoparticle characterization—prospects and limitations demonstrated on Au nanoparticles, Anal. Chim. Acta. 706 (2011) 367–378.
[28] W. Somchue, A. Siripinyanond, B.K. Gale, Electrical field-flow fractionation for metal nanoparticle characterization, Anal. Chem. 84 (2012) 4993–4998.
[29] J. Gigault, V.A. Hackley, Observation of size-independent effects in nanoparticle retention behavior during asymmetric-flow field-flow fractionation, Anal. Bioanal. Chem. 405 (2013) 6251–6258.
[30] D.-H. Tsai, Y.-F. Lu, F.W. DelRio, T.J. Cho, S. Guha, M.R. Zachariah, F. Zhang, A. Allen, V.A. Hackley, Orthogonal analysis of functional gold nanoparticles for biomedical applications, Anal. Bioanal. Chem. 407 (2015) 8411–8422.
[31] L. Liu, B. He, Q. Liu, Z. Yun, X. Yan, Y. Long, G. Jiang, Identification and accurate size characterization of nanoparticles in complex media, Angew. Chem. Int. Ed. 53 (2014) 14476–14479.
[32] M. Baalousha, B. Stolpe, J.R. Lead, Flow field-flow fractionation for the analysis and characterization of natural colloids and manufactured nanoparticles in environmental systems: a critical review, J. Chromatogr. A 1218 (2011) 4078–4103.
[33] H. Hagendorfer, R. Kaegi, M. Parlinska, B. Sinnet, C. Ludwig, A. Ulrich, Characterization of silver nanoparticle products using asymmetric flow field flow fractionation with a multidetector approach—a comparison to transmission electron microscopy and batch dynamic light scattering, Anal. Chem. 84 (2012) 2678–2685.
[34] H. Hinterwith, S.K. Wiedmer, M. Moilanen, A. Lehner, G. Allmaier, T. Waitz, W. Linder, M. Lämmerhofer, Comparative method evaluation for size and size-distribution analysis of gold nanoparticles, J. Sep. Sci. 36 (2013) 2952–2961.
[35] S. Gschwind, H. Hagendorfer, D.A. Frick, D. Günther, Mass quantification of nanoparticles by single droplet calibration using inductively coupled plasma mass spectrometry, Anal. Chem. 85 (2013) 5875–5883.
[36] C. Cascio, D. Gilliland, F. Rossi, L. Calzolai, C. Contado, Critical experimental evaluation of key methods to detect, size and quantify nanoparticulate silver, Anal. Chem. 86 (2014) 12143–12151.
[37] L. Pitkänen, A.M. Striegel, Size-exclusion chromatography of metal nanoparticles and quantum dots, Trends Anal. Chem. 80 (2016) 311–320.

[38] L. Trapiella-Alfonso, A.R. Montoro Bustos, J.R. Encinar, J.M. Costa-Fernandez, R. Pereiro, A. Sanz-Medel, New integrated elemental and molecular strategies as a diagnostic tool for the quality of water soluble quantum dots and their bioconjugates, Nanoscale 3 (2011) 954–957.
[39] F. Barahona, O. Geiss, P. Urbán, I. Ojea-Jimenez, D. Gilliland, J. Barrero-Moreno, Simultaneous determination of size and quantification of silica nanoparticles by asymmetric flow field-flow fractionation coupled to ICP-MS using silica nanoparticle standards, Anal. Chem. 87 (2015) 3039–3047.
[40] T.K. Mudalige, H. Qu, S.W. Linder, Asymmetric flow field-flow fractionation hyphenated ICP-MS as an alternative to cloud point extraction for quantification of silver nanoparticles and silver speciation: application for nanoparticles with a protein corona, Anal. Chem. 87 (2015) 7395–7401.
[41] B. Meermann, Field-flow fractionation coupled to ICP-MS: separation at the nanoscale, previous and recent application trends, Anal. Bioanal. Chem. 407 (2015) 2665–2674.
[42] D.M. Mitrano, A. Barber, A. Bednar, P. Westerhoff, C.P. Higgins, J.F. Ranville, Silver nanoparticle characterization using single particle ICP-MS (SP-ICP-MS) and asymmetrical flow field flow fractionation (AF4-ICP-MS), J. Anal. At. Spectrom. 7 (2012) 1131–1142.
[43] D. Mitrano, J. Ranville, K. Neubauer, R. Thomas, Field-flow fractionation coupled with ICP-MS for the analysis of engineered nanoparticles in environmental samples, Spectroscopy 27 (2012) 36–44.
[44] A.R. Montoro Bustos, J. Ruiz Encinar, A. Sanz-Medel, Mass spectrometry for the characterization of nanoparticles, Anal. Bioanal. Chem. 405 (2013) 5637–5643.
[45] A.M. Striegel, Multiple detection in size-exclusion chromatography of macromolecules, Anal. Chem. 77 (2005) 104A–113A.
[46] A.M. Striegel, W.W. Yau, J.J. Kirkland, D.D. Bly, Modern Size-Exclusion Liquid Chromatography: Practice of Gel Permeation and Gel Filtration Chromatography, 2nd ed., Wiley, Hoboken, NJ, 2009.
[47] A.R. Montoro Bustos, E.J. Petersen, A. Possolo, M.R. Winchester, *Post hoc* interlaboratory comparison of single particle ICP-MS size measurements of NIST gold nanoparticle reference materials, Anal. Chem. 87 (2015) 8809–8817.
[48] RM reports of investigation found online: www.nist.gov/srm; Reference Material 8011, Gold Nanoparticles, Nominal 10 nm Diameter; National Institute of Standards and Technology, Gaithersburg, MD.
[49] RM reports of investigation found online: www.nist.gov/srm; Reference Material 8012, Gold Nanoparticles, Nominal 30 nm Diameter; National Institute of Standards and Technology, Gaithersburg, MD.
[50] RM reports of investigation found online: www.nist.gov/srm; Reference Material 8013, Gold Nanoparticles, Nominal 60 nm Diameter; National Institute of Standards and Technology, Gaithersburg, MD.
[51] SRM certificates of analysis found online at: www.nist.gov/srm. (a) Standard Reference Material 3121, Gold (Au) Standard Solution. (b) Standard Reference Material 3124, Indium (In) Standard Solution; National Institute of Standards and Technology, Gaithersburg, MD.
[52] G.R. McGowan, M.A. Langhorst, Development and application of an integrated high-speed, computerized hydrodynamic chromatograph, J. Colloid Interface Sci. 89 (1982) 94–106.
[53] A.K. Brewer, A.M. Striegel, Particle characterization by quadruple-detector hydrodynamic chromatography, Anal. Bioanal. Chem. 393 (2009) 295–302.
[54] A.K. Brewer, A.M. Striegel, Hydrodynamic chromatography of latex blends, J. Sep. Sci. 33 (2010) 3555–3563.
[55] A.K. Brewer, A.M. Striegel, Characterizing a spheroidal nanocage drug delivery vesicle using multi-detector hydrodynamic chromatography, Anal. Bioanal. Chem. 399 (2011) 1507–1514.
[56] A.M. Striegel, Thermodynamic equilibrium of the solute distribution in size-exclusion chromatography, J. Chromatogr. A 1033 (2004) 241–245.
[57] Size-exclusion chromatography, in: A.M. Striegel, S. Fanali, P.R. Haddad, C.F. Poole, P. Schoenmakers, D. Lloyd (Eds.), Liquid Chromatography: Fundamentals and Instrumentation, Elsevier, Amsterdam, 2013, pp. 193–223.
[58] A.M. Striegel, Size-exclusion chromatography: smaller, faster, multi-detection, and multi-dimensions, Anal. Bioanal. Chem. 390 (2008) 303–305.
[59] A.M. Striegel, Longitudinal diffusion in size-exclusion chromatography: a stop-flow size-exclusion chromatography study, J. Chromatogr. A 932 (2001) 21–31.
[60] A.M. Striegel, Hydrodynamic chromatography: packed columns, multiple detectors, and microcapillaries, Anal. Bioanal. Chem. 402 (2012) 77–81.
[61] A.M. Striegel, A.K. Brewer, Hydrodynamic chromatography, Annu. Rev. Anal. Chem. 5 (2012) 15–34.
[62] A.K. Brewer, A.M. Striegel, Characterizing the size, shape, and compactness of a polydisperse prolate ellipsoidal particle *via* quadruple-detector hydrodynamic chromatography, Analyst 136 (2011) 515–519.
[63] S.L. Isenberg, A.K. Brewer, G.L. Côté, A.M. Striegel, Hydrodynamic versus size exclusion chromatography characterization of alternan and comparison to off-line MALS, Biomacromolecules 11 (2010) 2505–2511.
[64] A.K. Brewer, A.M. Striegel, Characterizing string-of-pearls colloidal silica by multidetector hydrodynamic chromatography and comparison to multidetector size-exclusion chromatography, off-line multiangle static light scattering, and transmission electron microscopy, Anal. Chem. 83 (2011) 3068–3075.
[65] G. Stegeman, J.C. Kraak, H. Poppe, Dispersion in packed-column hydrodynamic chromatography, J. Chromatogr. 634 (1993) 149–159.
[66] K. Proulx, K.J. Wilkinson, Separation detection and characterization of engineered nanoparticles in natural waters using hydrodynamic chromatography and multi-method detection (light scattering, analytical ultracentrifugation and single particle ICP-MS), Environ. Chem. 11 (2014) 392–401.
[67] K. Proulx, M. Hadioui, K.J. Wilkinson, Separation, detection and characterization of nanomaterials in municipal wastewaters using hydrodynamic chromatography coupled to ICPMS and single particle ICPMS, Anal. Bioanal. Chem. 408 (2016) 5147–5155.
[68] M. Roman, C. Rigo, H. Castillo-Michel, I. Munivrana, V. Vindigni, I. Mičetić, F. Benetti, L. Manodori, W.R.L. Cairns, Hydrodynamic chromatography coupled to single-particle ICP-MS for the simultaneous characterization of AgNPs and determination of dissolved Ag in plasma and blood of burn patients, Anal. Bioanal. Chem. 408 (2016) 5109–5124.
[69] L. Pitkänen, A.M. Striegel, Determining the core, corona, and total size of CdSeS/ZnS quantum dots by SEC/QELS and TEM, Anal. Bioanal. Chem. 408 (2016) 4003–4010.
[70] B.J. Berne, R. Pecora, Dynamic Light Scattering with Applications to Chemistry, Biology, and Physics, Dover, Mineola, NY, 2000.
[71] C.S. Johnson Jr., D.A. Gabriel, Laser Light Scattering, Dover, New York, 1981.
[72] J.P. Wilcoxon, J.E. Martin, F. Parsapour, B. Wiedenman, D.F. Kelley, Photoluminescence from nanosize gold clusters, J. Chem. Phys. 108 (1998) 9137–9143.
[73] S. López-Sanz, N. Rodríguez Fariñas, R. Serrano Vargas, R. d. C. Rodríguez Martín-Doimeadios, Á. Ríos, Methodology for monitoring gold nanoparticles and dissolved gold species in culture medium and cells used for nanotoxicity tests by liquid chromatography hyphenated to inductively coupled plasma-mass spectrometry, Talanta 164 (2017) 451–457.
[74] J.P. Wilcoxon, J.E. Martin, P. Provencio, Size distributions of gold nanoclusters studied by liquid chromatography, Langmuir 16 (2000) 9912–9920.
[75] J.P. Wilcoxon, J.E. Martin, P. Provencio, Optical properties of gold and silver nanoclusters investigated by liquid chromatography, J. Chem. Phys. 115 (2001) 998–1008.
[76] J.P. Wilcoxon, P. Provencio, Etching and aging effects in nanosize Au clusters investigated using high-resolution size-exclusion chromatography, J. Phys. Chem. B 107 (2003) 12949–12957.
[77] J.P. Wilcoxon, P. Provencio, Heterogeneous growth of metal clusters from solutions of seed nanoparticles, J. Am. Chem. Soc. 126 (2004) 6402–6408.
[78] J. Liu, K.E. Murphy, R.I. MacCuspie, M.R. Winchester, Capabilities of single particle inductively coupled plasma mass spectrometry for the size measurement of nanoparticles: a case study on gold nanoparticles, Anal. Chem. 86 (2014) 3405–3414.
[79] F. Laborda, E. Bolea, J. Jiménez-Lamana, Single particle inductively coupled plasma mass spectrometry: a powerful tool for nanoanalysis, Anal. Chem. 86 (2014) 2270–2278.

SUPPORTING INFORMATION

Quantitative characterization of gold nanoparticles by size-exclusion and hydrodynamic chromatography, coupled to inductively coupled plasma mass spectrometry (SEC/ICP-MS and HDC/ICP-MS) and quasi-elastic light scattering (HDC/QELS)

Leena Pitkänen[a], Antonio R. Montoro Bustos, Karen E. Murphy, Michael R. Winchester,*

André M. Striegel*

Chemical Sciences Division, National Institute of Standards and Technology (NIST), 100 Bureau Drive, Gaithersburg, MD 20899, USA

[a]Current address: Department of Food and Environmental Sciences, University of Helsinki, P.O. Box 27, 00014 Helsinki, Finland

*To whom correspondence should be addressed. MRW e-mail: mwinchester@nist.gov, AMS e-mail: andre.striegel@nist.gov

Choice of eluent and column packing material in SEC/ICP-MS and HDC/ICP-MS

The main challenges for performing quantitative size-based chromatographic NP separations are two-fold: First, a mobile phase or carrier fluid must be found in which the NPs remain suspended but do not aggregate with each other to an appreciable extent (as is the case in polymer science, temperature is considered an implicit parameter when discussing the mobile phase/carrier fluid). Second, a combination of mobile phase/carrier fluid and stationary phase must be found wherein the sample elutes by a predominantly entropic mechanism (solution conformational entropy in the case of SEC, solution translational entropy in the case of HDC) [1, 2], with minimal enthalpic contributions to the separation.

It has been shown in various studies that an HDC eluent originally developed by McGowan and Langhorst for polystyrene (PS) and butadiene copolymer latexes can be successfully applied to the multi-detector HDC analysis of PS and poly(methyl methacrylate) latexes as well as to terbium(III) chloride nanoparticles with a “cage-like” structure [3-5]. Here, a variation on this eluent was employed in both the SEC and HDC Au NP separations. Details of the eluent itself are given in the Experimental – SEC/ICP-MS section. The rationale behind this seemingly complex eluent is as follows: The non-ionic surfactant Triton X-100 is used to prevent analyte aggregation in solution, whereas SDS, an anionic surfactant, is employed to prevent analyte sorption onto the column packing material (more on the choice of material follows below). Formaldehyde is used for its bactericidal properties, and sodium hydrogen phosphate helps maintain the slightly basic pH of the separations. A basic pH is needed with the particular column packing material used, sulfonated styrene/divinyl benzene (for both SEC and HDC separations, as mentioned earlier), because the sulfonation reaction is reversible at acidic pH. (It

should be noted that very recent results, by Ruiz-Cabello *et al.* [6], indicate that a basic pH also helps to maintain a repulsive force between PS particles in aqueous solution). Previous success employing this column packing material in the above-mentioned multi-detector HDC analyses led us to hypothesize that, with an appropriately formulated eluent, sulfonated styrene/divinyl benzene could be a good choice of column packing material for size-based Au NP separations. Additionally, reports in the literature attest to the sorption of NPs onto both silica-based and non-functinalized polymeric SEC packing materials [7, 8]. The fact that dilute suspensions of Au NPs are considered stable (especially as compared to, *e.g.*, aqueous silver NP suspensions, which typically suffer from changes in size due to dissolution in water related to the release of silver ions from the NP surface), and that the NPs are both non-functionalized (*i.e.*, do not possess an organic corona) and can be considered to behave as hard spheres in solution, all indicate that NP morphology should not be affected by the SEC or HDC separations.

To summarize what was mentioned above, two challenges need to be dealt with, namely preventing analyte aggregation in solution (or suspension) and preventing analyte sorption onto the chromatographic column packing. To determine whether or not aggregation has occurred, we rely on the on-line quasi-elastic light scattering detector. The response of this detector is directly proportional to the molar mass of the analyte [1, 9]. All things being equal, an aggregate of particles will have a higher molar mass than will the individual, unaggregated particles. It is this very feature which makes on-line light scattering detectors ideal for the determination of analyte aggregation in solution: The separation system separates the aggregated from the unaggregated particles (in SEC or HDC, the larger aggregates elute earlier than do the unaggregated particles; the opposite is generally true in AF4 and related separations), while the response from the light scattering detector indicates whether a particular peak does or does not correspond to an

aggregate [1, 9-12]. In the HDC/QELS analyses, no extraneous peaks other than those of the analytes appear present nor is there any other indication of analyte aggregation in solution. As has been already stated, SEC/QELS analyses were not possible with the particular columns employed. However, given that the chemistry of the HDC and SEC packing materials is identical and that the same eluent was used in both cases, the conclusions from HDC/QELS should be inductively applicable to the SEC analyses.

It should be noted that, prior to the experiments with sulfonated styrene/divinyl benzene columns, we also performed experiments employing SEC columns packed with non-functionalized styrene/divinyl benzene particles. Employing aqueous eluents consisting, individually, of 0.02 % NaN_3 and of 5 mmol L^{-1} sodium dodecyl sulfate, either no peaks were observed or a multiplicity of very small *S*/*N* peaks were seen to elute from the columns. The low *S*/*N*, as well as the absence of any peaks, is indicative of column sorption by the analytes, and the on-line static light scattering detector showed that the earlier eluting peaks in the group resulted from Au NP aggregation in solution.

HDC/QELS autocorrelation functions

Figure S1 shows the autocorrelation functions, obtained at the apexes of the HDC chromatograms, for the 10 nm, 30 nm, and 60 nm Au NPs. As can be seen, all autocorrelation functions are exponential and, in all cases, the R^2 value between the experimental data and a single exponential decay function are ≥ 0.997. Where not visible, error bars on experimental data points are smaller than the data markers themselves.

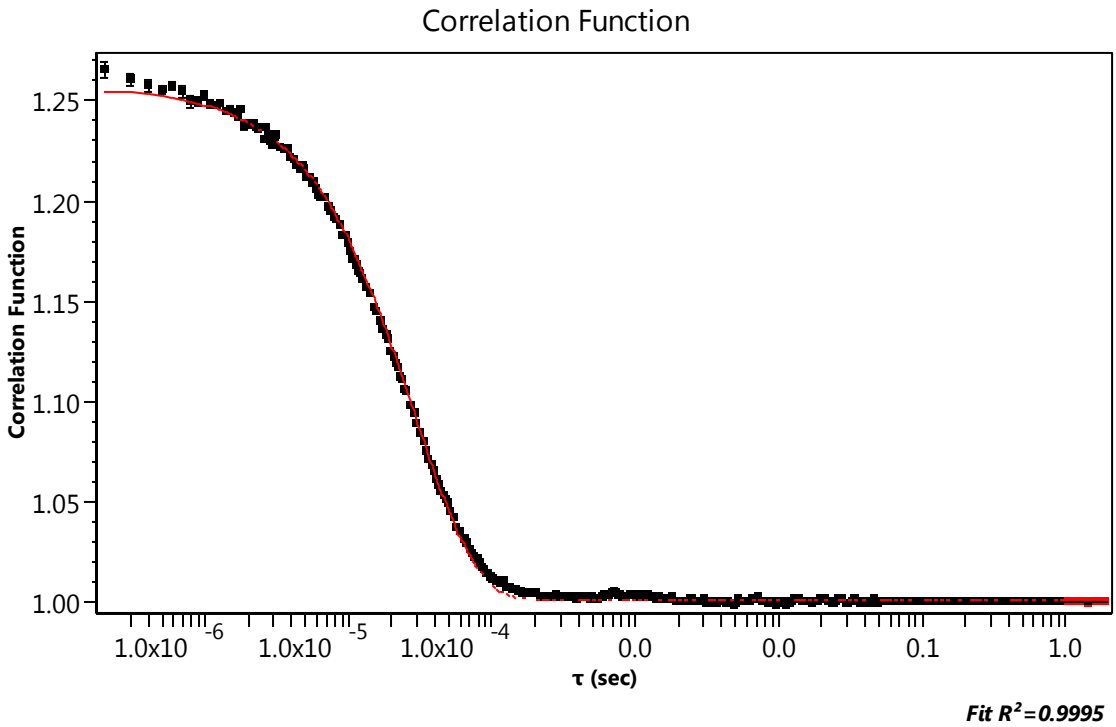
Correlation Function
Correlation Function
1.25
1.20
1.15
1.10
1.05
1.00
1.0x10 -6
1.0x10 -5
1.0x10 -4
0.0
0.0
0.1
1.0
τ (sec)
Fit R²=0.9995

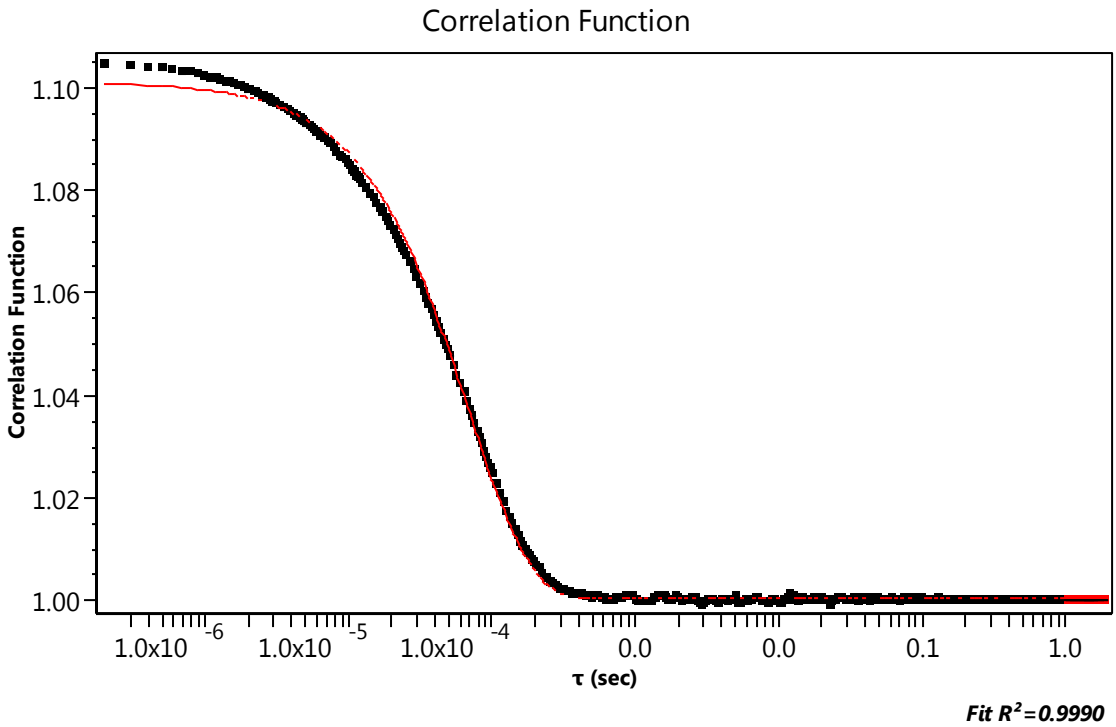
Correlation Function
Correlation Function
1.10
1.08
1.06
1.04
1.02
1.00
1.0x10 -6
1.0x10 -5
1.0x10 -4
0.0
0.0
0.1
1.0
τ (sec)
Fit R²=0.9990

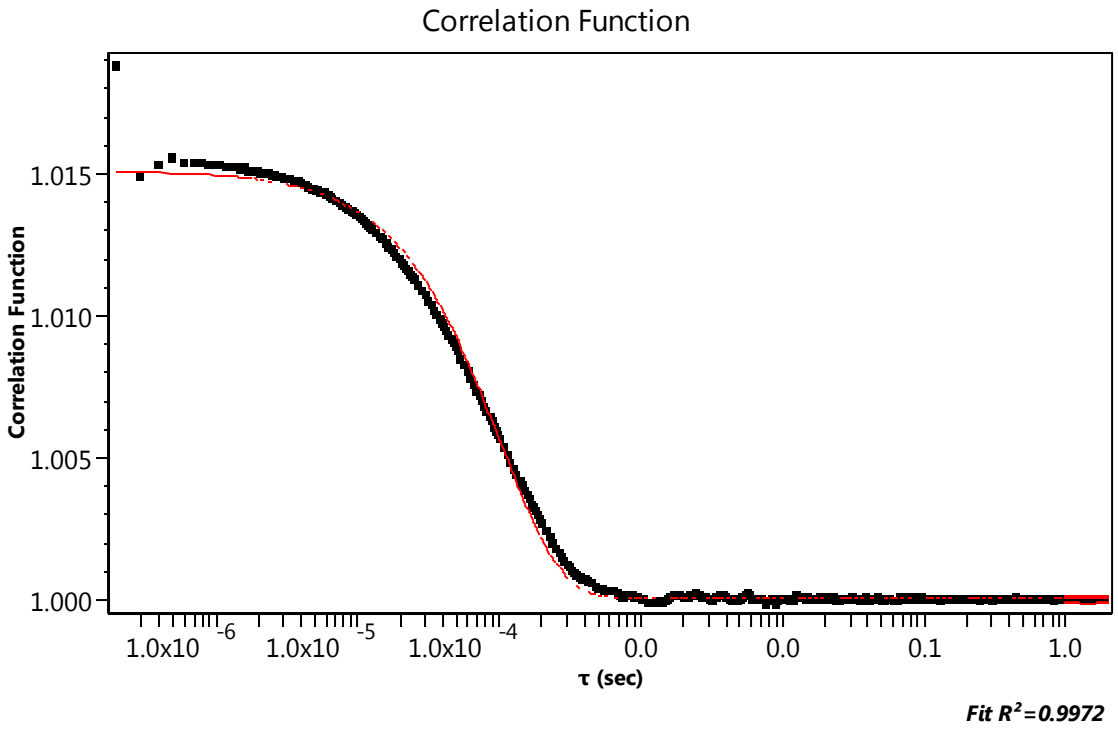

Figure S1. QELS autocorrelation functions, for chromatographic slices eluting at the peak apexes during on-line HDC/QELS experiments. Top: 10 nm Au NP; middle: 30 nm Au NP; bottom: 60 nm Au NP. Black squares indicate experimental data, with accompanying standard deviations; where no error bars are shown, standard deviations are smaller than data markers. Red lines indicates single exponential fits to the data.

REFERENCES

[1] A. M. Striegel, W. W. Yau, J. J. Kirkland, D. D. Bly, Modern Size-Exclusion Liquid Chromatography: Practice of Gel Permeation and Gel Filtration Chromatography, 2nd ed., Wiley, Hoboken, NJ, 2009.

[2] A. M. Striegel, A. K. Brewer, Hydrodynamic chromatography, Annu. Rev. Anal. Chem. 5 (2012) 15-34.

[3] A. K. Brewer, A. M. Striegel, Particle characterization by quandruple-detector hydrodynamic chromatography, Anal. Bioanal. Chem. 393 (2009) 295-302.

[4] A. K. Brewer, A. M. Striegel, Hydrodynamic chromatography of latex blends, J. Sep. Sci. 33 (2010) 3555-3563.

[5] A. K. Brewer, A. M. Striegel, Characterizing a spheroidal nanocage drug delivery vesicle using multi-detector hydrodynamic chromatography, Anal. Bioanal. Chem. 399 (2011) 1507-1514.

[6] F. J. M. Ruiz-Cabello, T. Oncsik, M. A. Rodríguez-Valverde, P. Maroni, M. Cabrerizo-Vilchez, Specific ion effects and pH dependence on the interaction forces between polystyrene particles, Langmuir 32 (2016) 11918-11927.

[7] F. Liu, G. Wei, Effect of mobile-phase additives on separation of gold nanoparticles by size-exclusion chromatography, Chromatographia 59 (2004) 115-119.

[8] J. P. Wilcoxon, P. P. Provencio, Chemical and optical properties of CdSe and CdSe/ZnS nanocrystals investigated using high-performance liquid chromatography, J. Phys. Chem. B 109 (2005) 13461-13471.

[9] T. H. Mourey, SEC molecular-weight-sensitive detection, Int. J. Polym. Anal. Charac. 9 (2004) 97-135.

[10] A. M. Striegel, Multiple detection in size-exclusion chromatography of macromolecules, Anal. Chem. 77 (2005) 104A-113A.

[11] A. M. Striegel, J. D. Timpa, Size exclusion chromatography of polysaccharides in dimethylacetamide-lithium chloride, in Strategies in Size Exclusion Chromatography, M. Porschka, P. L. Dubin, eds., ACS Symp. Ser. 635, American Chemical Society, Washington, DC, 1996, pp. 366-378.

[12] A. M. Striegel, Viscometric detection in size-exclusion chromatography: Principles and select applications, Chromatographia 79 (2016) 945-960.